Vol. 06, No. 2 (2024) 513-522, doi: 10.24874/PES06.02.009

Proceedings on Engineering Sciences

www.pesjournal.net

TENSILE STRENGTH, SURFACE MORPHOLOGY, AND PRELIMINARY CORRELATION ANALYSIS OF AL-17SI ALLOYS IN FRICTION STIR WELDING PROCESSES

Shailesh Rao A.[1]
Somaiah C. A.
Yuvaraj Naik

Received 14.09.2023.
Received in revised form 19.11.2023.
Accepted 29.12.2023.
UDC – 621.791.76/.79

Keywords:

Friction Stir Welding, Microstructure, Tensile, Fracture Surface, Correlation Studies

A B S T R A C T

This study examines the intricate dynamics of the Friction Stir Welding (FSW) process utilized on the challenging hypereutectic composition of Al-17Si alloys, which obstructs effective metal flow and mixing. Higher rotating speeds stimulate greater mixing, but lower rotational speeds (600 rpm) cause uneven metal circulation around the tool. The benefits of increasing rotation speed to 1200 rpm for stress and strain outweigh the disadvantages for tensile strength. The ideal tensile strength is reached at lower feed rates (50mm/min), in conjunction with precise plunging depth, ensuring consistent extrusion and material flow to produce fine Si particles. Shear forces brought on by uneven metal flow around the tool pin are what give the fracture surface its distinctive knife-edge characteristics; sharper edges appear at higher feed rates. Additionally, this work makes use of correlation and regression analysis to shed light on the complex relationships between important process variables and material characteristics, highlighting the essential components that control the FSW process for Al-17Si alloys. To optimize the FSW process and subsequently enhance joint quality and performance, these findings emphasize the significance of carefully choosing process parameters such as tool rotation, feed rates, and plunging force.

1. INTRODUCTION

Friction stir welding (FSW) is a popular joining procedure in a variety of manufacturing industries, particularly for aluminum alloys used in defense, vehicle, and aerospace applications. Weld joint strength is determined by elements such as tool rotational speed, material strength, and motor power (Debroy & Bhadeshia, 2010; Murr, 2010). The author (Yigezu et al., 2014) highlighted the relevance of correct stirring action in creating a fine grain microstructure in the nugget zone, which adds to the weld joint's tensile strength for Al 12Si alloys. To ensure satisfactory weld quality and mechanical

[1] Corresponding author: Shailesh Rao A.
Email: shailesh.rao@nmit.ac.in

qualities during testing, heat dissipation during the welding process should result in plastic deformation, gradual cooling, and movement around the tool probe (Cui et al., 2014; Liu et al., 2004). As demonstrated during welding of Al6013 alloys (Heinz & Skrotzki, 2007, Abbass & Sharhan, 2023), post-weld heat treatment can also improve weld strength. Heat distribution in FSW processes has been studied using mathematical modelling, with some studies comparing the results to actual processes and highlighting difficulties (Kim et al., 2010; Song & Kovacevic, 2003; Nandan et al., 2007). Microstructure and mechanical characteristics of 6xxx, 5xxx, and 7xxx series alloys have been extensively researched during FSW operations (Ravichandran et al., 2016; Guo et al., 2014; Peel et al., 2003; Milenkovic et al., 2021, Ali & Saffar, 2022).

FSW can be used to join metals in the different aluminum alloys (Shailesh et al., 2017). The ideal strength was attained in Yuqing Mao's research on the FSW of 2060 Al-Li thin alloy plates with a tool rotation of 1180rpm and feed rate of 118mm/min. Welding speed and tool rotation speed were also studied for their effects on quality, microstructure, phase particle change, and mechanical properties. While The author studied the mechanical properties of welded AC4A aluminium alloy plates, finding better mechanical properties in the weld nugget and thermo-mechanically affected zone (TMAZ) areas (Mao et al., 2015), Ali and Saffar (2022) studied the effects of several process parameters on the FSW of aluminum alloy plates, including tool axial force, transverse force, torque, and temperature. According to E. Sukedai's study of the microstructural features of Al-Mg-Si (6061-T6Al) alloy during FSW (Sukedai, 2019), the strain hardening rate was greater than that of the base material.

One of the most important aspects of FSW is the welding speed or feed rate, which determines how long the welding tool remains in contact with the material. By slowing down, more time is spent with the tool's shoulder in contact with the workpiece, leading to a stronger weld. For instance, in T6 and T4 temper conditions, M. Ericson (Ericson, 2003) investigated the fatigue strength of Al-Mg-Si alloy 6082 friction stir welded joints. He found that compared to TIG and MIG welded joints, FSW joints exhibited greater fatigue strength. The shorter contact time between the workpiece and the electrode in TIG welding is likely responsible for the superior fatigue performance of TIG over MIG. As a result of its effect on heat production, plastic deformation, and material mixing, the rotating speed of the tool is also crucial in FSW. The author claims that the rotational and longitudinal speeds of the tool have a major impact on the weld joint's grain formation and mechanical behaviour (James, 2003). A high tensile strength and elongation were achieved in the stirred zone weld joint at the optimal rotational speed.

In FSW, the weld quality and other properties are defined by the tool profile. Cylindrical, tapered, square, and threaded tool profiles are only some of the options for joining metal components. To investigate the impact of the pin profile on several process parameters, Shailesh (Shailesh et al., 2017) fabricated friction welded joints of aluminum plates. He discussed the quality and mechanical properties of the weld joint are profoundly affected by several variables in FSW, including welding speed, tool rotation speed, and tool profile. To make a welding connection that is strong and durable, it is necessary to maximize these characteristics.

Friction Stir Welding's material flow theory was the most challenging to grasp because of the intense heat interaction between the tool shoulder and the workpiece. Copper foils placed between welded joints as tracing material is one of the ways explored in the literature for studying material flow behaviour. Copper is used, but W powder is also used to learn about metal flow in the process. To investigate the metal flow behaviour of copper and W particles on A6061- T6 aluminium sheets, Yuan- Ching Lin et al. (2013) employed a powder tracing technique. Triangular pins had their gaps filled because of the unidirectional flow of material. The alloy was driven downward using a screw-threaded instrument, creating uniform mixing between the bottom and upper sheets.

For the appropriate mechanical properties to be achieved in Friction Stir Welding, knowledge of the material's flow behaviour is essential. By optimizing welding parameters and tool shape, better mechanical qualities can be achieved in welded joints.

2. EXPERIMENTAL DETAILS

In the experiments, the billets with dimensions of 150 x 60 x 6mm is utilized. The joining process was conducted with specific process parameters, including a plunging force of 25kN, three feed rates (50, 100, and 150mm/min), and three tool rotations (600, 900, and 1200rpm). The tool employed in the process was made of H13 hot die steel, had a shoulder diameter of 20mm, a height of 25mm, and a tool pin taper from φ6 to φ4mm. The microstructures were examined using standard image analyzer equipment, while tensile strength testing was carried out on specimens cut according to ASTM standards using a BIS nano UTM.

2.1 Appearance of the Weld Morphology

Figure 1 depicts the varied weld patterns seen throughout different FSW techniques due to metal flow variances. The hard material did not help to move the tool considerably downwards at a reduced rotating speed of 600rpm and a feed rate of 50mm/min, and some diffused material spread around the weld surface. The discontinuous deformed

material ejected from the RS side traveled across the hot weld surface forming micro weld over the weld region. As shown in Fig. 1, increasing the tool rotation to 900 and 1200rpm resulted in more diffused material coming out of the RS weld zone and a greater amount of diffused material entangled on the weld surface during motion. Increasing the feed rate to 100mm/min reduced heat input, and at higher tool rotations (900 and 1200rpm), there was little diffusion. However, a limited quantity of material was moved over the weld surface and collected as discontinuous defects in the AS region. At a feed rate of 150mm/min, there were voids in the weld joint during tool rotation at 900rpm and no joining of the alloy during tool rotation at 1200rpm. Increased tool rotation increased alloy dispersion, with metal transport dependant on the severity of the alloy's deformation. Silicon particles in the alloys limited deformation during 600rpm tool rotation, making diffusion problematic. As a result, metal flow was interrupted on the RS side of the weld zone. With tool rotation at 900rpm, high friction and heat input were created, lessening the restriction of silicon particles on metal transport, and resulting in discontinuous metal transport with a greater amount of diffused material adhering to the weld surface. As the rotational speed was increased to 1200rpm, more diffused material emerged from the RS zone and deposited in the AS region, as seen in Fig. 1. The adhesion time decreased as the tool feed rate increased, and while metal moved easily from the RS to the AS side, defects were visible on the AS side of the weld. The production of defects increased with tool feed rate, and connecting the alloys was challenging at a feed rate of 150mm/min. The chosen plunging force did not aid in the proper stirring and diffusing of the alloys, resulting in voids and faulty joints visible in the surface morphology during the process.

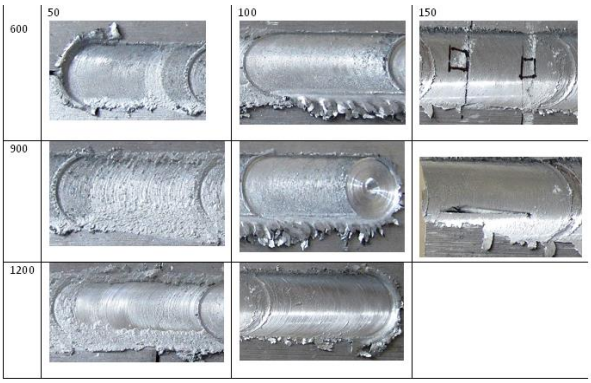

Figure 1. Surface Morphology for various tool rotation and tool feed rate

2.2 Tensile Strength

The transverse tensile strength of the weld joint was determined for various process conditions. Changes in process parameters were demonstrated to have a considerable impact on the tensile strength of the welding joint. Adequate alloy mixing during the FSW is more difficult to achieve with slower tool rotation and feed rates. The alloy's tensile strength is decreased by this dislocation, and it may even fracture at the nugget-TMAZ junction. By raising the tool rotation rate, which softens the alloys in the material, a slight increase in tensile strength is attained. Here the viscosity rises due to the presence of silicon, the alloy in the nugget zone becomes softer and the joint starts to become flexible.

The tensile strength of the alloys with different rotational speeds is shown in Figure 2. Here the tool typically has difficulty in plugging between the edge of the alloy. This is mostly due to the significant amount of friction and thrust force applied to the device during the process. When the tool rotated at 600 revolutions per minute, and the feed rate was 50 mm/min, the plunging depth was found to be 4.22mm deep. This is because the plastically deformed alloy rotates around the tool periphery with relatively little shear force, allowing the scattered alloy to appear as powders. It is evident from this that inserting the tool between the welding joints is a difficult process.

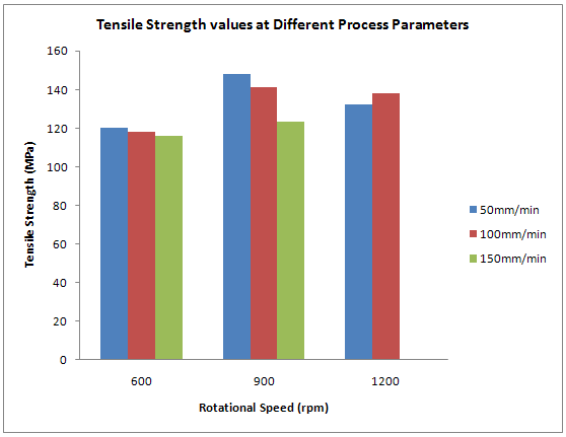

Figure 2. Tensile strength value during various machining parameters during FSW process

As the tool's rotational speed increases, the plunging depth, on the other hand, reduces as the rotation speed and feed rate are increased to 900 revolutions per minute (rpm) and 50, 100, and 150 mm/min respectively, Figure 3. This results in a gradual smoothing out of the surface. According to this evidence, a higher rotational speed combined with a lower feed rate may produce a welding surface finish that is of a higher quality. Due to differences in the relative velocity between the dispersed layers, the tool has difficulty dispersing the alloy when the rotation speed is increased to 1200 rpm, which causes it to have difficulty diffusing the alloy. The upshot of this is a subpar weld joint due to the inconsistency in the tool position maintained throughout the connecting of the hard components.

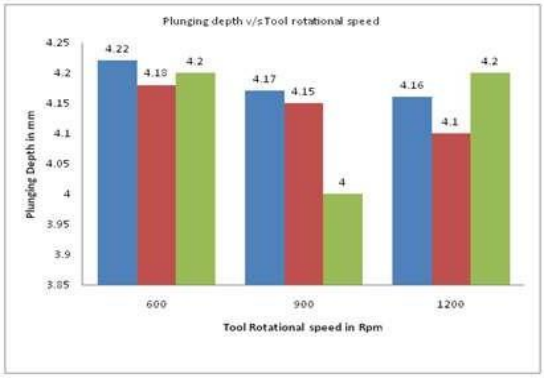

Figure 3. Ploughing Depth during various machining parameters during FSW process

Overall, it is possible to conclude that the difficulty in plunging and mixing scattered alloy can result in the creation of fewer faults on the weld surface. Understanding the diffusion process during weld joining might be aided by the surface roughness of the weld surface. A greater rotational speed and lower feed rate may result in a better weld surface finish as seen from Figure 4. However, an erratic tool position during hard material joining may result in a poor weld connection.

Overall, Friction Stir Welding (FSW) technique is separated into two stages: plunging and dwelling and welding, which work together to form a strong welding connection.

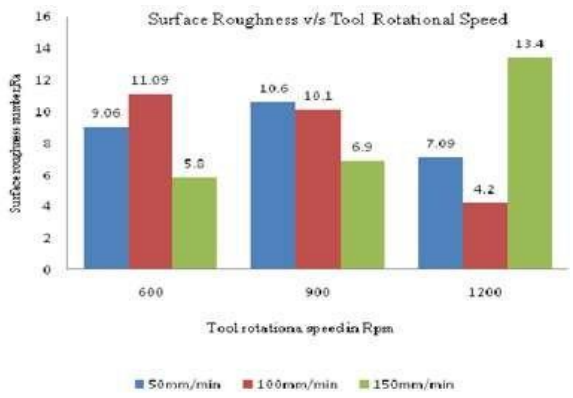

Figure 4. Surface roughness value during various machining parameters during FSW process

The FSW tool rotates and plunges into the weld gap between the two workpieces during the plunging and dwelling phase. Heat is generated by the friction between the tool and the workpieces, which increases as the tool rotation speed increases. The material softens and loses strength as it heats up, allowing the tool to penetrate deeper. If the material is tougher, it may resist softening and cause shear stress between the tool circumference and the disseminated material. Furthermore, the push force prevents the tool from moving downward. As a result, the tool advances to a particular depth, generating transient heat in the weld zone.

During the dwell period, the revolving tool generates more heat, raising the weld temperature even higher. During this phase, the substance diffuses and expands significantly. The heat input and the combination of tool rotation and feed rate determine the alloy's state, whether semi-plastic or plastic. During the welding phase, a transverse feed is employed to distort the alloy's leading edge. Depending on the process settings, the tool rotation softens and mixes these alloys. The distributed alloy in both weld zones correctly mixes during the optimum process, which improves weld quality. However, inappropriate joining can occur when the tool is rotated quickly and/or the tool traverse feed is increased. Inadequate relative motion of the diffused material around the tool rotation, inappropriate diffusion during the process due to less adhesion between the tool and workpiece, and difficulty in inserting soft material in the weld gap after the tool motion can all lead to faulty joining.

Top of Form
Top of Form
According to the study's findings, the FSW process generates higher heat due to mechanical friction at high tool rotation (900rpm) and low feed rate (50mm/min). This heat leads the alloy to enter a plastic condition, reducing its strength dramatically. As the alloy softens, it penetrates deeper into the material and rotates with changing shear stress around the tool circumference, resulting in poor heat transfer and the creation of demarcations between the nugget and TMAZ zones. The alloy's silicon presence is advantageous because it increases the solidification rate, forcing powdered defects to travel from the RS to AS side and adhere to the hot weld surface, forming micro welds during the plunge and dwell phase. However, the silicon particle's restriction on plastic deformation softens the TMAZ zone while smoothing the demarcations between the zones.
More heat is generated when the tool rotation is raised to 1200rpm, resulting in the formation of big powdery defects that spread across the weld surface. During tool retraction at a lower tool rotation of 600rpm, the plastic deformation of the alloy transfers between the weld sides and generates continuous defects on the weld surface. On the reduced feed rate of the traverse feed, the leading edge of the alloy diffuses significantly. Because of the increase in solidification rate caused by silicon nucleation, placing the alloy in the weld gap may be challenging, contributing to the formation of powdery defects over the weld zone.

Small dislocations of grains are visible in the TMAZ and nugget zone, showing that the alloy did not soften during the process. According to the research, at a low tool spin of 600rpm, the heat input is balanced, making the material soft during the plunging force and causing it to travel deeper downwards. The

TMAZ zone has little alloy diffusion, whereas the nugget zone has considerable diffusion.

The study discovered that the tool's rotating speed had a substantial impact on welding quality. When the rotational speed is raised, the alloy undergoes intensive mixing, which ultimately decides the weld quality (Maa et al., 2006). Tunnel flaws are developed because of anomalous stirring at higher feed rates and tool rotation speeds above 900rpm (Jayaram & Balasubramanian, 2013; Kim et al., 2006). When fine Si particles develop in the nugget zone, the tensile strength of the weld joint improves. However, because of the production of clusters of shattered Silicon particles during high spinning rates, coarse Si grains diminish tensile strength (Milenkovic et al., 2021). The researchers discovered that a tool rotation speed of 900rpm and a feed rate of 50mm/min resulted in excellent tensile strength due to optimal heat input, which allows for proper churning and the creation of tiny silicon grains in the nugget zone. However, increasing the tool rotation to 1200rpm resulted in the creation of voids in the TMAZ zone and a loss in tensile strength.

As the tool feed rate increases, the adhesion between the tool and the disseminated alloys becomes more problematic. Although the alloys' deformation remains constant during the plunging and dwelling periods, the diffusion process begins to change during the traversing feed. The alloy is forced to diffuse and migrate about the tool circumference during the welding process, resulting in sliding between the soft material and the tool circumference. This reduces adhesion and strain rate, causing the diffused alloy to move away from the retarding side surface. However, no severe plastic deformation occurred, and the scattered material that consistently landed on the RS side of the weld zone had no significant distortion. As the rotating speed increased, some alloy deformation occurred, and it migrated uniformly from the RS to the AS of the weld joint. The alloys, however, did not soften as the input rate rose, making diffusion difficult. Even though some joining happened during the process, proper mixing did not take place, and the weld gap was obvious. The alloy did not join at 1200rpm due to the inability to mix the alloy and rub the weld gap surface. There was some diffusion in this location, but no friction bonding. Because of the poor adherence, it was difficult for the alloys to soften. The microstructure revealed demarcation near the TMAZ and nugget zone, as expected. Due to the extreme deformation of the alloy and insufficient heat transmission throughout the operation, fine grains containing primary silicon formed in the nugget zone. Inadequate heat transfer could be attributed to a decrease in strain rate and unequal relative velocity between the diffused alloys revolving around the tool perimeter. The alloy softened as the tool rotation increased, and minor deformation with fine grains was seen in the TMAZ zone. The diffused material in the weld gap consolidated promptly during the tool rotation at 1200rpm and feed rate of 150mm/min, and fine granules were visible on its surface.

Figure 5 exhibits the stress-strain graphs for Al-17Si alloys at various process parameters showing that hypereutectic alloys have difficulty plunging the tool at reduced tool rotation, and the yield stresses for the process vary between 20 and 30 MPa. However, as the tool rotation speed increases, the plunging depth and alloy mixing improve, resulting in some strain during the tensile stress. Despite this improvement, the yield stress remains in the 20 to 25 MPa range. An increase in tool rotation to 1200 rpm results in even more stress and strain reduction. Nonetheless, a loss in tensile strength is observed across all methods.

An increase in silicon content has a negative impact on both weld surface formation and tensile strength. Mixing hypereutectic alloys can be difficult due to poor plunging depth induced by the material's enhanced strength, which results in thrust during tool plunging. Despite these obstacles, the technique allows for some alloy mixing, resulting in a strong connection between the alloys.

Figure 6 shows the cracked surface observed during FSW procedures, which demonstrated the presence of flaws due to discontinuous shear strain across the tool circle. As a result, multiple plastic deformations occurred at various locations within the weld zone. Poor metal circulation was seen above the tool pin during tool rotation at 600rpm for the Al-17Si alloy, with better circulation at the shoulder. This resulted in non-uniform metal circulation around the tool's perimeter, resulting in two sharp, knife-edged metals on the fracture surface. Shear between the welding locations owing to uneven metal circulation around the tool pin could have caused the fracture. The sharpness of the fracture surface grew as the feed rate rose.

Because of the increased input rate during FSW, it was difficult to adequately stir or mix the alloys. The rate of heat generation during the thermal cycle reduced as the feed rate increased. According to the author (Razal et al., 2011), the amount of plastic development per unit time during transverse feed is highly dependent on tensile strength. Proper dispersion of silicon particles is also required for increased tensile strength. The current investigation discovered that the best tensile strength for Al-17Si alloy was obtained at a lower feed rate of 50mm/min. Because a proper plunging depth extruded and circulated the material in a uniform direction, fine Si particles formed, which continued with further tool input. Increased tool feed rate disrupted alloy mixing, resulting in the production of coarse Si particles in the TMAZ zone. A crack was initiated during the tensile

testing procedure on Al-17Si alloys, resulting in a fracture. For most of the alloys, there was no diffusion of the alloy on the cracked surface. However, when tool rotation increased, some improvement in alloy mixing was noticed, resulting in a slight rise in strength values. The detailed insights into the fracture studies conducted on the sample are observed in the literature (Shailesh et al.,2023).

Rotational Speed, in (RPM)	Al-17Si Feed rate (in mm/min)		
	50	100	150
600	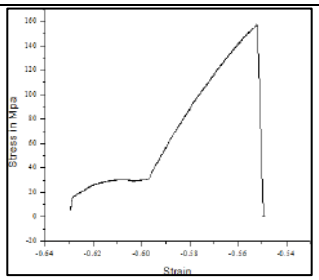 (a)	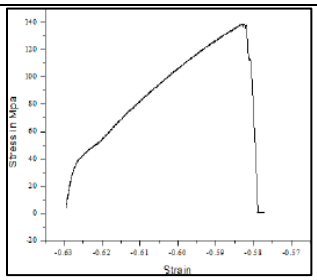 (b)	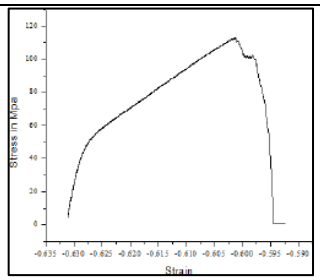 (c)
900	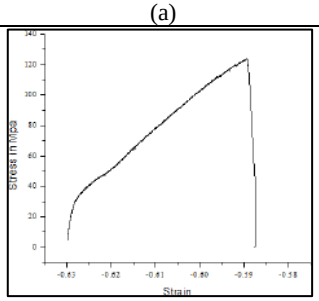 (d)	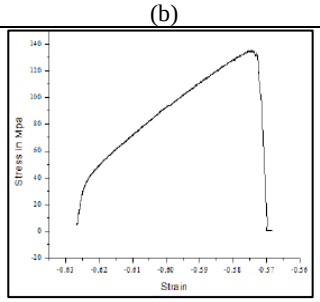 (e)	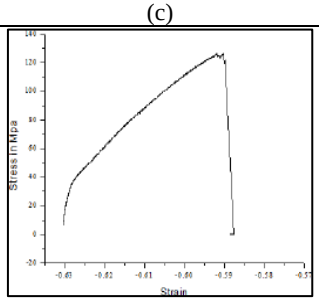 (f)
1200	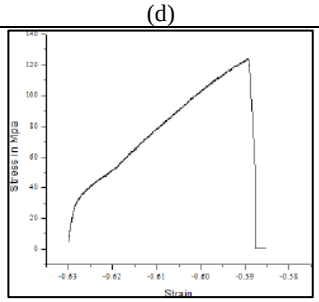 (g)	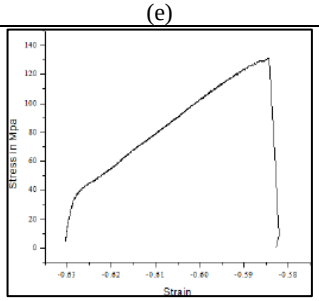 (h)	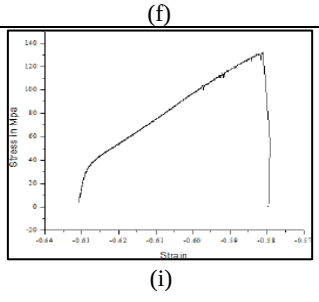 (i)

Figure 5. Stress Strain Diagram for all the process parameter

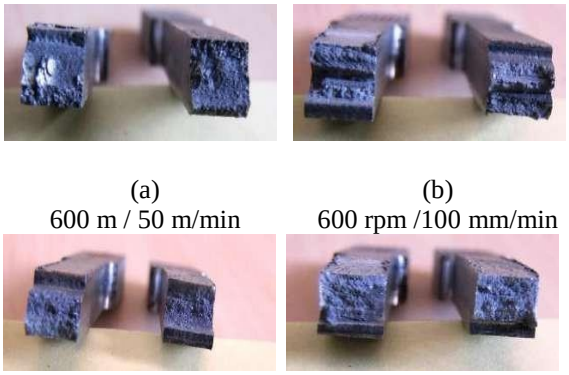

(a) 600 m / 50 m/min

(b) 600 rpm /100 mm/min

(c) 900 rpm / 50 mm/min

(d) 900 rpm /100 m/min

Figure 6. Samples with fractured surface after tensile test

2.3 Correlation and Regression

Within the domain of correlation testing, the correlation coefficient (r) plays a crucial role in evaluating the magnitude and direction of the relationship between two numerical variables. The correlation coefficient, which measures the strength and direction of the relationship between variables, is a numerical value that ranges from -1 to 1. The present study utilized the Spearman method to systematically assess the associations between key process parameters and their respective output variables. The investigation in this study employed the computational framework of R programming, which is widely recognized for its statistical functionalities.

The subsequent analysis of correlation revealed significant findings. It is worth noting that there was a significant negative correlation of -0.67 observed

between tool rotation and material hardness. This finding suggests that an increased level of tool rotation resulted in a noticeable reduction in material hardness during the Friction Stir Welding (FSW) process. The discovery serves to highlight the crucial significance of tool rotation in the process of tailoring material properties. Furthermore, the observed correlation coefficient of -0.43 between the feed rate and tensile strength provides evidence of a negative relationship. Specifically, an increase in the feed rate was shown to be associated with a subsequent decrease in the tensile strength. This finding serves as a sobering reminder of the crucial need for prudent feed rate selection in attaining precise tensile characteristics. The data also revealed a negative correlation of -0.43 between feed rate and material hardness, which supports the notion that feed rate significantly influences both tensile strength and material hardness.

The regression analysis performed with R software produced useful predictive models for key parameters in the Friction Stir Welding (FSW) process. These models shed light on the connections between process factors and crucial material attributes. The three predictive models were created with the R program and are displayed below:

- Surface Roughness = 13.294 + (0.03 Feed Rate) - (0.007 Tool Rotation).
- Tensile Strength = 138.02 - (0.57 x Feed rate + 0.007 x Tool Rotation)
- Hardness = 33.70 minus (0.03 x Feed rate) minus (0.006 x Tool Rotation).

In Al-17Si alloy Friction Stir Welding (FSW), this regression equation quantifies the relationship between process parameters and surface roughness. The feed rate, according to this equation, increases surface roughness. This demonstrates that increasing the feed rate causes the tool to move quickly along the surface, potentially increasing tool-surface interactions, and surface defects. Higher tool rotation, on the other hand, reduces surface roughness. This implies that raising the rotational speed of the tool may smooth tool movement and increase surface quality.

The negative link between feed rate and tensile strength in the regression equation for tensile strength shows a key dynamic. As the feed rate increases, it presents specific conditions during the welding process that may result in a decrease in the tensile strength of the material. These phenomena could be attributable to reasons such as increased heat generation or altered material flow dynamics, which could result in microstructural changes that affect the mechanical characteristics of the material. In contrast, the positive connection between tool rotation and tensile strength indicates a significant effect. Increased tool rotation rates result in increased tensile strength, meaning that raising the tool's rotational speed improves the integrity and strength of the ensuing weld connection. This could be due to more efficient material mixing and consolidation at greater tool rotation rates, which results in a more robust and structurally sound welded interface.

The regression equation for Hardness discovered a negative association between feed rate and hardness. Increased feed rate introduces specific variables during the welding process that contribute to material hardness reduction. This could be related to changes in material flow dynamics and increased heat input. These changes may cause variations in the microstructure, altering the hardness qualities of the material. Similarly, the inverse relationship between tool rotation and hardness shows yet another important influence. Increased tool rotation rates result in a modest reduction in material hardness. This shows that raising the tool's rotational speed changes material hardness, possibly due to factors associated to material consolidation and grain refining at higher rotation rates.

These findings have important implications for FSW process optimization. Engineers can modify feed rate and tool rotation strategically based on the unique hardness needs of a certain application. They can then customize the welding process to meet the appropriate material hardness qualities, hence improving the overall performance and durability of the welded joints. However, while this model gives useful insights, its usefulness may be limited by factors like material composition, tool shape, and process parameters. As a result, it is advised that this model be validated and maybe refined in specific operational scenarios during future studies.

3. CONCLUSIONS

The following are the conclusions from the above work:

- The Friction Stir Welding (FSW) technique for Al-17Si alloys has illuminated its hypereutectic composition's problems. Metal circulation and mixing were poor, especially at lower tool revolutions (600rpm), resulting in 20-25 MPa tensile strength. Increasing tool rotation to 1200rpm reduced stress and strain but decreased tensile strength across all processes.
- The high silicon component in Al-17Si alloys affected weld surface formation and tensile strength. Quantifying process parameter-material property interactions required correlation and regression analysis. These investigations showed that higher tool rotation and lower feed rates affected material hardness and tensile strength.

- At 50mm/min, precision plunging depth allowed consistent extrusion and material circulation, producing tiny Si particles and optimal tensile strength. In contrast, increasing tool feed disrupted alloy mixing, resulting in coarser Si particles in the TMAZ.
- The correlation and regression analyses reveal complicated connections between process parameters and material properties in Friction Stir Welding (FSW) for Al-17Si alloys. The -0.67 relationship between tool rotation and hardness shows it impacts material hardness. Tool rotation reduces material hardness, emphasizing its role in property adjustment. Feed rate negatively influences tensile strength and hardness (-0.43). This highlights the importance of feed rate selection for tensile and material hardness.
- The regression equations formalized these correlations, giving satisfied mathematical models for parameter selection. These equations allow us to understand the quantitatively tune the FSW process for surface roughness, tensile strength, and hardness. Correlation and regression analysis helps in optimizing FSW parameters and improving Al-17Si alloy welded connections.

Acknowledgment: The author extends their appreciation to the management and Principal of Nitte Meenakshi Institute of Technology, Bangalore, for their invaluable financial support in conducting the research.

References:

Abbass, M. K., & Sharhan, N. a. B. (2023). Characteristics of AL6061-SIC-AL2O3 surface hybrid composites fabricated by friction stir processing. Journal of Materials and Engineering, 1(4), 147–158. https://doi.org/10.61552/jme.2023.04.002

Ali, S. M., & Q. Al Saffar, I. (2022). Effect of SiO2 and B4C nanoparticles hybrid addition on mechanical properties of AA6061-T6 surface composite via friction stir processing. *Tribology in Industry, 44*(4), 687–695. https://doi.org/10.24874/ti.1312.05.22.09

Cui, G. R., Ni, D. R., Ma, Z. Y., & Li, S. X. (2014). Effects of friction stir processing parameters and in situ passes on microstructure and tensile properties of Al-Si-Mg casting. *Metallurgical and Materials Transactions A, 45*(12), 5318–5331. https://doi.org/10.1007/s11661-014-2494-8

DebRoy, T., & Bhadeshia, H. K. D. H. (2010). Friction stir welding of dissimilar alloys – a perspective. *Science and Technology of Welding and Joining, 15*(4), 266–270. https://doi.org/10.1179/174329310x12726496072400

Ericsson, M. (2003). Influence of welding speed on the fatigue of friction stir welds, and comparison with MIG and TIG. *International Journal of Fatigue, 25*(12), 1379–1387. https://doi.org/10.1016/s0142-1123(03)00059-8

Guo, J., Chen, H., Sun, C., Bi, G., Sun, Z., & Wei, J. (2014). Friction stir welding of dissimilar materials between AA6061 and AA7075 Al alloys effects of process parameters. *Materials & Design (1980-2015), 56*, 185–192. https://doi.org/10.1016/j.matdes.2013.10.082

Heinz, B., & Skrotzki, B. (2002). Characterization of a friction-stir-welded aluminum alloy 6013. *Metallurgical and Materials Transactions B, 33*(3), 489–498. https://doi.org/10.1007/s11663-002-0059-5

James, M. (2003). Weld tool travel speed effects on fatigue life of friction stir welds in 5083 aluminium. *International Journal of Fatigue, 25*(12), 1389–1398. https://doi.org/10.1016/s0142-1123(03)00061-6

Jayaraman, M., & Balasubramanian, V. (2013). Effect of process parameters on tensile strength of friction stir welded cast A356 aluminium alloy joints. *Transactions of Nonferrous Metals Society of China, 23*(3), 605–615. https://doi.org/10.1016/s1003-6326(13)62506-6

Jovicic, G., Milosević, A., Šokac, M., Santosi, Z., Kočović, V., Šimunović, G., & Vukeli, D. (2023). The modelling of surface roughness after the turning of Inconel 601 by using artificial neural network. Journal of Materials and Engineering, 1(4), 179–188. https://doi.org/10.61552/jme.2023.04.006

Kim, W. K., Goo, B. C., & Won, S. T. (2010). Optimal design of friction stir welding process to improve tensile force of the joint of A6005 extrusion. *Materials and Manufacturing Processes, 25*(7), 637–643. https://doi.org/10.1080/10426910903365745

Kim, Y., Fujii, H., Tsumura, T., Komazaki, T., & Nakata, K. (2006). Effect of welding parameters on microstructure in the stir zone of FSW joints of aluminum die casting alloy. *Materials Letters, 60*(29–30), 3830–3837. https://doi.org/10.1016/j.matlet.2006.03.123

Lin, Y. C., Liu, J. J., & Chen, J. N. (2013). Material flow tracking for various tool geometries during the friction stir spot welding process. *Journal of Materials Engineering and Performance, 22*(12), 3674–3683. https://doi.org/10.1007/s11665-013-0680-2

Liu, H. J., Fujii, H., & Nogi, K. (2004). Microstructure and mechanical properties of friction stir welded joints of AC4A cast aluminium alloy. *Materials Science and Technology, 20*(3), 399–402. https://doi.org/10.1179/026708304225012279

Ma, Z., Sharma, S., & Mishra, R. (2006). Effect of multiple-pass friction stir processing on microstructure and tensile properties of a cast aluminum–silicon alloy. *Scripta Materialia, 54*(9), 1623–1626. https://doi.org/10.1016/j.scriptamat.2006.01.010

Mao, Y., Ke, L., Liu, F., Huang, C., Chen, Y., & Liu, Q. (2015). Effect of welding parameters on microstructure and mechanical properties of friction stir welded joints of 2060 aluminum lithium alloy. *The International Journal of Advanced Manufacturing Technology, 81*(5–8), 1419–1431. https://doi.org/10.1007/s00170-015-7191-2

Milenkovic, S., Zivic, F., Jovanovic, Z., Radovanovic, A., Ljusic, P., & Grujovic, N. (2021). Review of friction stir processing (FSP) parameters and materials for surface composites. *Tribology in Industry, 43*(3), 470–479. https://doi.org/10.24874/ti.1169.06.21.08

Muigai, M. N., Mwema, F. M., Akinlabi, E. T., Jen, T., Fatoba, O. S., Leso, T. P., & Mphasha, P. (2022). TIG Welding Methods of Repairing Steel Components with Stainless Steel Coatings. *Tribology in Industry, 44*(3), 434–448. https://doi.org/10.24874/ti.1177.08.21.04

Murr, L. E. (2010). A review of FSW research on dissimilar metal and alloy systems. *Journal of Materials Engineering and Performance, 19*(8), 1071–1089. https://doi.org/10.1007/s11665-010-9598-0

Nandan, R., Roy, G., Lienert, T., & Debroy, T. (2007). Three-dimensional heat and material flow during friction stir welding of mild steel. *Acta Materialia, 55*(3), 883–895. https://doi.org/10.1016/j.actamat.2006.09.009

Peel, M., Steuwer, A., Preuss, M., & Withers, P. (2003). Microstructure, mechanical properties and residual stresses as a function of welding speed in aluminium AA5083 friction stir welds. *Acta Materialia, 51*(16), 4791–4801. https://doi.org/10.1016/s1359-6454(03)00319-7

Rao, A. G., Ravi, K. R., Ramakrishnarao, B., Deshmukh, V. P., Sharma, A., Prabhu, N., & Kashyap, B. P. (2012). Recrystallization phenomena during friction stir processing of hypereutectic aluminum-silicon alloy. *Metallurgical and Materials Transactions A, 44*(3), 1519–1529. https://doi.org/10.1007/s11661-012-1489-

Ravichandran, M., Thirunavukkarasu, M., Sathish, S., & Anandakrishnan, V. (2016). Optimization of welding parameters to attain maximum strength in friction stir welded AA7075 joints. *Materials Testing, 58*(3), 206–210. https://doi.org/10.3139/120.110838

Razal Rose, A., Manisekar, K., & Balasubramanian, V. (2011). Influences of welding speed on tensile properties of friction stir welded AZ61A magnesium alloy. *Journal of Materials Engineering and Performance, 21*(2), 257–265. https://doi.org/10.1007/s11665-011-9889-0

Root, J., Field, D., & Nelson, T. (2009). Crystallographic texture in the friction-stir-welded metal matrix composite Al6061 with 10 vol pct Al2O3. *Metallurgical and Materials Transactions A, 40*(9), 2109–2114. https://doi.org/10.1007/s11661-009-9883-4

Shailesh Rao, A., & Yuvaraja, N. (2017). Comparison of appearance, microstructure and tensile properties during friction stir welding processes of Al–Si alloys. *Physics of Metals and Metallography, 118*(7), 716–722. https://doi.org/10.1134/s0031918x17070092

Shailesh Rao, A., Yuvaraja, N. (2023). Impact of Welding parameters on diffusion, surface formation temperature and tensile strength of Al 17Si alloys, COMADEM, 6(23), 25-31, 2023

Song, M., & Kovacevic, R. (2003). Thermal modeling of friction stir welding in a moving coordinate system and its validation. *International Journal of Machine Tools and Manufacture, 43*(6), 605–615. https://doi.org/10.1016/s0890-6955(03)00022-1

Sukedai, E., & Yokoyama, T. (2012). A study on microstructure and strain-hardening rate of friction stir welded Al-Mg-Si alloys using a weak beam technique. *Journal of Physics: Conference Series, 371*, 012083. https://doi.org/10.1088/1742-6596/371/1/012083

Yigezu, B. S., Venkateswarlu, D., Mahapatra, M., Jha, P., & Mandal, N. (2014). On friction stir butt welding of Al + 12Si/10 wt%TiC in situ composite. *Materials & Design (1980-2015), 54*, 1019–1027. https://doi.org/10.1016/j.matdes.2013.09.034

Shailesh Rao A.
Nitte Meenakshi Institute of Technology, Yelahanka, Bangalore-64 India
shailesh.rao@nmit.ac.in
ORCID 0000-0001-6190-9857

Somaiah C. A.
Nitte Meenakshi Institute of Technology, Yelahanka, Bangalore-64 India
somaiah_01@yahoo.co.in
ORCID 0009-0001-1694-0211

Yuvaraja Naik
Presidency University, Rajanukunte, Bangalore
y.naik_75@gmail.com
ORCID 0009-0001-0804-3254